Science of the Total Environment 593–594 (2017) 571–580

Contents lists available at ScienceDirect

Science of the Total Environment

journal homepage: www.elsevier.com/locate/scitotenv

Biofilm structures (EPS and bacterial communities) in drinking water distribution systems are conditioned by hydraulics and influence discolouration

K. Fish [a,b,*], A.M. Osborn [c], J.B. Boxall [a]

[a] Pennine Water Group, Department of Civil and Structural Engineering, The University of Sheffield, Sheffield S1 3JD, UK
[b] NERC Biomolecular Analysis Facility, Department of Animal and Plant Sciences, Western Bank, Sheffield S10 2TN, UK
[c] Biosciences and Food Technology Discipline, School of Science, RMIT University, PO Box 71, Bundoora, Melbourne VIC3083, Australia

HIGHLIGHTS

- Analysis of drinking water biofilm physical structure and bacterial communities
- Biofilms developed naturally in full-scale drinking water distribution facility.
- Hydraulic conditions influence cohesive strength of EPS.
- Biofilm structure differs between Varied Flow and Steady State conditioned biofilms.
- Understanding biofilms, including EPS, is key to safeguarding water quality.

GRAPHICAL ABSTRACT

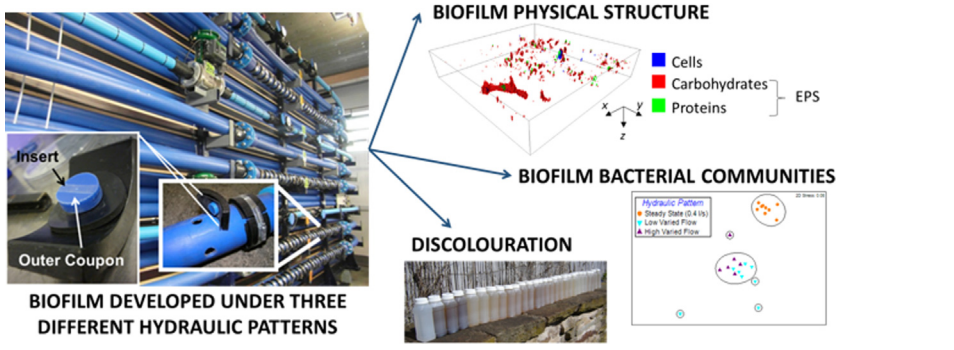

ARTICLE INFO

Article history:
Received 31 January 2017
Received in revised form 13 March 2017
Accepted 19 March 2017
Available online xxxx

Editor: Simon Pollard

Keywords:
Drinking water distribution systems
Biofilms
Extracellular polymeric substances (EPS)
Hydraulic patterns
Water quality
Terminal-restriction fragment length polymorphism (T-RFLP)

ABSTRACT

High-quality drinking water from treatment works is degraded during transport to customer taps through the Drinking Water Distribution System (DWDS). Interactions occurring at the pipe wall-water interface are central to this degradation and are often dominated by complex microbial biofilms that are not well understood. This study uses novel application of confocal microscopy techniques to quantify the composition of extracellular polymeric substances (EPS) and cells of DWDS biofilms together with concurrent evaluation of the bacterial community. An internationally unique, full-scale, experimental DWDS facility was used to investigate the impact of three different hydraulic patterns upon biofilms and subsequently assess their response to increases in shear stress, linking biofilms to water quality impacts such as discolouration. Greater flow variation during growth was associated with increased cell quantity but was inversely related to EPS-to-cell volume ratios and bacterial diversity. Discolouration was caused and EPS was mobilised during flushing of all conditions. Ultimately, biofilms developed under low-varied flow conditions had lowest amounts of biomass, the greatest EPS volumes per cell and the lowest discolouration response. This research shows that the interactions between hydraulics and biofilm physical and community structures are complex but critical to managing biofilms within ageing DWDS infrastructure to limit water quality degradation and protect public health.

1. Introduction

Drinking water treatment works are routinely used to provide safe drinking water and protect public health. The quality of water leaving

* Corresponding author at: Pennine Water Group, Department of Civil and Structural Engineering, The University of Sheffield, Sheffield S1 3JD, UK.
E-mail address: K.fish@sheffield.ac.uk (K. Fish).

http://dx.doi.org/10.1016/j.scitotenv.2017.03.176

treatment works is generally high and complies to (inter)national quality standards which set aesthetic and health-based limits for the presence of various micro-(biological) chemical and physical parameters. Treated water is then transported to consumers through Drinking Water Distribution Systems (DWDS) which are complex, heterogenic pipe networks with a vast surface area-to-volume ratio (11 m^2:1 m^3 calculated for UK systems (Fish et al., 2016)). DWDS act as biological and physico-chemical reactors changing and degrading water quality during transport.

Globally, water discolouration is the leading example of aesthetic degradation occurring within DWDS (Ginige et al., 2011; Vreeburg and Boxall, 2007), which may also mask other, less-visible quality failures. The processes driving the accumulation and mobilisation of discolouration material have been attributed to the formation and subsequent release of cohesive-layers that attach to the pipe wall at strengths influenced by the pipeline specific hydraulic conditions (Boxall and Saul, 2005; Husband et al., 2008). These layers are mobilised when the imposed hydraulic forces exceed the conditioning force (Boxall and Saul, 2005) which in DWDS could occur following a burst or an increase in demand.

Microbial (especially biofilm) ecology is emerging as a key determinant in the formation and behaviour of layers on pipe surfaces (Fish et al., 2016; Husband et al., 2016). Biofilms are assemblages of microbial cells embedded within a complex matrix of extracellular polymeric substances (EPS) which comprises (primarily) carbohydrates and proteins (lipids and extracellular DNA have also been detected but at lower concentrations; (Flemming and Wingender, 2010, 2001)) with (in)organics, including metals, potentially incorporated (Neu and Lawrence, 2009; Zacheus et al., 2001). EPS constitutes the most extensive part of a biofilm and has many functions, including providing structure and mechanical stability (Neu and Lawrence, 2009). The hydraulics imposed during biofilm development are thought to influence accumulation/detachment and also condition adhesive/cohesive strength. While various studies have begun to investigate these processes, these are rarely conducted within the context of DWDS (Vieira and Melo, 1999; Beyenal and Lewandowski, 2002; Purevdorj et al., 2002; Simões et al., 2005).

In DWDS, biofilms are exposed to hydraulic variations, which influence boundary-layer hydraulics and exchange mechanisms (e.g. distribution of inorganics and planktonic cells) at the pipe wall. DWDS typically experience a double-peaked diurnal hydraulic pattern with a low flow (or stagnant) period overnight. However, much of the previous research regarding hydraulic and biofilm interactions has investigated steady state flow rates, rather than varied flow (VF) patterns (Purevdorj et al., 2002; Rochex et al., 2008; Simões et al., 2003). It has been shown in several such idealised bench-top studies that if the shear stress applied exceeds the strength of the EPS, biofilm will be mobilised (Lehtola et al., 2006). Biofilm mobilisation in real systems could engender public health- and/or drive water quality-failures, due to the detachment of cells and (in)organics concentrated in the EPS. Such mobilisation is directly analogous to the cohesive-layer theory of discolouration (Husband et al., 2016).

The impact that hydraulics have upon conditioning a biofilm to resist detachment (and hence cause water quality issues) is still debated (Abe et al., 2012; Lehtola et al., 2006; Percival et al., 1999; Simões et al., 2005). Some studies have found that greater turbulent flows during growth can condition biofilms to be more resistant to detachment (Percival et al., 1999), others have found the reverse (Abe et al., 2012). It has been concluded that the changes in biofilm characteristics under diverse shear stresses are due to different mechanical requirements to resist external forces and avoid detachment (Beyenal and Lewandowski, 2002; Purevdorj et al., 2002; Vieira and Melo, 1999). However, these results cannot necessarily be directly scaled-up and applied to real DWDS as the hydraulics, biofilm development and bulk-phase chemistry within the model systems are unrepresentative of full-scale DWDS. Additionally, these studies cannot determine the driving factor behind biofilm accumulation or conditioning, which could be average flow rate, peak (maximum) flow rate, low flow rate or flow variation. To address the aforementioned issues an internationally unique, full-scale DWDS test facility has been established at The University of Sheffield, providing an accurate replication of operational DWDS hydraulics using different flow patterns and enabling laboratory-level control of biofilm sampling (Deines et al., 2010; Douterelo et al., 2013; Fish et al., 2015; Sharpe, 2012). Research using this facility has begun to assess the impact of hydraulic pattern upon water quality (Sharpe, 2012) and bacterial diversity (Douterelo et al., 2013) but crucially has not incorporated the interactions between hydraulics and the EPS. Further understanding of the hydraulics-biofilm (EPS and microbial community)-water quality interactions is essential so that biofilm formation and detachment processes can be better understood to more effectively manage and safeguard drinking water quality and hence public health. This is particularly important as infrastructure ages and DWDS must cope with increasing and changing water demand associated with population growth and climate change.

This study aimed to determine the impact of Steady State (SS), Low Varied Flow (LVF) and High Varied Flow (HVF) hydraulic regimes on the quantity and composition of EPS and cells (referred to as physical structure) of DWDS biofilms, as well as on variation in biofilm bacterial community structure. Additionally, we aimed to investigate the effect of elevated shear stress (pipe flushing) on the potentially different biofilm structures and to quantify changes in associated discolouration of water.

2. Materials and methods

2.1. Biofilm growth and hydraulic regimes

Biofilms were developed at 16 °C (representative of UK summer pipe water temperatures) for 28 days within a full-scale, temperature controlled DWDS experimental facility (Fig. 1), described in detail in Fish et al. (2015). This system replicated the hydraulics (including boundary-layer hydraulics), water chemistry, microbiology and exchange mechanisms of operational DWDS while enabling laboratory level control of environmental parameters and sampling regime. The facility comprised three 203 m long loops of high-density polyethylene, 79.3 mm in internal diameter, with each loop representing an independent experimental replicate (i.e. n = 3). Pipe loops contained multiple

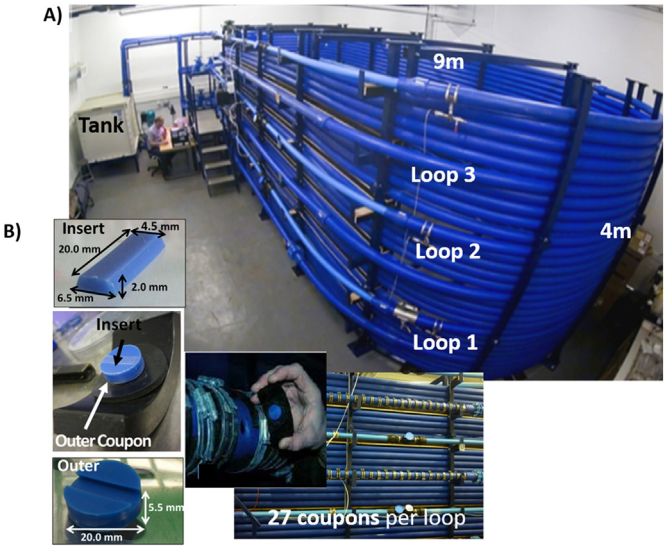

Fig. 1. Drinking Water Distribution system (DWDS) test facility. A) Pipe facility, with total volume of 4.5 m^3 comprising a 1.53 m^3 tank and 3 loops of 200 m long, 79.9 mm internal diameter high density polyethylene pipe into which Pennine Water Group (PWG) coupons (Deines et al., 2010) were inserted (B) to allow sampling of internal pipe wall surfaces, which comprised an insert for microscopy analysis and an outer coupon for molecular analyses, dimensions as indicated.

apertures into which Pennine Water Group (PWG) coupons (Deines et al., 2010) were inserted to provide a removable surface for sampling of internal biofilms (Fig. 1). Water from the local DWDS (sourced from surface waters) was supplied directly to the facility from the trunk main and pumped around the loops from an enclosed reservoir tank with a system retention time of 24 h (i.e. a trickle turnover). Three consecutive hydraulic experiments were undertaken, with three replications of each. In each hydraulic experiment, water was pumped around each of the three loops of the system (i.e. triplicates were conducted for each experiment) following one of the three hydraulic patterns shown in Fig. 2 – Steady State (SS), Low Varied Flow (LVF) or High Varied Flow (HVF). The entire system was hyper-chlorinated between each hydraulic test and coupons were sterilised (Fish et al., 2015).

To investigate the importance of average, minimum and maximum flow rates in shaping biofilm structure and stability each regime was designed to have the same average flow rate (0.4 ls^{-1}) but different peak (maximum) and low flows (Fig. 2). LVF and HVF regimes were based upon field data from real DWDS but designed to have the same "night time" flow (0.23 ls^{-1}, 0.25 Nm^{-2}) with different peak flow rates (0.54 ls^{-1}, 0.34 Nm^{-2} for LVF and 0.75 ls^{-1}, 0.40 Nm^{-2} for HVF), to provide an insight into the importance of the low flow and peak flow periods in influencing biofilm structure.

Various water quality parameters (Table S1) were monitored throughout each experiment (triplicates were taken weekly). In all cases biofilms were sampled at Day 0 (sampled 60–90 min after commencing the flow pattern of the experiment; taken for comparison with Day 28 to confirm material accumulation) and Day 28 for each experiment (n = 9 each time point, with three coupons per loop sampled without draining the system). The insert of the PWG coupon was used to analysis biofilm physical structure, via confocal microscopy and the outer part was used for molecular analysis of biofilm bacterial community structure, as we describe previously (Fish et al., 2015).

2.2. Biofilm exposure to elevated shear stress

Following the development phase of each of the hydraulic tests (SS, LVF or HVF) biofilms were exposed to a series of three increasing shear stresses (0.42, 1.75 and 2.91 Nm^{-2}) by flushing each loop of the facility independently (detailed description in Douterelo et al., 2013) at three increasing flow rates (0.80, 3.20 and 4.50 ls^{-1}) for three turnovers (i.e. the time taken for the loop volume of water to be circulated three times). The same water quality parameters monitored during growth (Table S1) were monitored (n = 3) throughout the flushing phase of each experiment (SS, LVF and HVF). In particular, iron and manganese (analysed via the ICPOES method, AlControl Laboratories, UK) were measured after one turnover to detect material mobilisation into the water column before dilution and determine any discolouration response (these metals have been shown to be responsible for discolouration) to the elevated shear stress occurring at the pipe wall. Biofilm samples were taken at the end of the flushing phase (n = 9, three from each loop) for each hydraulic test (SS, LVF or HVF).

2.3. Physical structure analysis

Confocal laser scanning microscopy (CLSM) and digital image analysis (DIA) were used to characterise the physical structure of Day 28, Post-flush and Day 0 biofilms (only brief Day 0 results are reported as little material was present). A detailed description of this method is provided in Fish et al. (2015). In brief, the inserts (n = 5, selected as a subset of the n = 9 due to time constraints) were fixed in 5% formaldehyde for 48 h and rinsed in phosphate buffer solution (PBS). The fixed biofilm samples and controls (sterile inserts, n = 3) were then stained with SYTO 63 to target cells, fluorescein-5-isothiocyanate (FITC) to target proteins and Concanavalin-A tetramethylrhodamine (Con-A) to target carbohydrates (all stains from Molecular Probes, California, USA). It should be acknowledged that Syto 63 stains intracellular as well as extracellular nucleic acids (e.g. Böckelmann et al., 2006). However, extracellular DNA in EPS has been reported at very low concentrations and, as is suggested in Ivleva et al. (2009), it is likely to be present in concentrations below the limit of detection of staining methods (if present at all). Therefore the Syto 63 stained nucleic acids are hereafter referred to in terms of cells. Carbohydrates and proteins were stained as these are the predominant components of the EPS (Flemming and Wingender, 2001; Gao et al., 2008; Wang et al., 2014).

Lambda-Z-stack images of the triple stained biofilms (and controls) were generated for five Fields of View (FOV) per sample, using an LSM510 meta upright CLSM with a ×20 EC Plan Neofluar objective (0.5 NA) and unmixed to remove autofluorescence using LSM510 software (Kroto Imaging Facility, The University of Sheffield, UK). Subsequently, DIA was used to median filter the images to reduce noise; threshold the images (threshold values: SYTO 63 – 2401, FITC – 1701, and Con-A– 1701); overlay and render unmixed images (including generating 3D images); calculate physical structure parameters and analyse the resultant data set (Fish et al., 2015). A combination of Python v2.7.2 (www.python.org) and R v2.15 (R Development Core Team, 2008) were used for this analysis. The physical structure parameters which were calculated were the volume (μm^3 per μm^2 area of biofilm) of each stained component (and subsequently the EPS – proteins plus carbohydrates- and the total biofilm-EPS plus cells-volumes); EPS-to-cell ratio and carbohydrate-to-protein ratio to assess composition (volume of the first parameter was divided by the second). A parameter termed spread was used as a proxy for thickness as explained in Fish et al. (2015) and finally, peak location, which was the location in the Z-stack at which the greatest density of carbohydrates and/or proteins was present relative to that of the cells.

2.4. Community structure analysis

Bacterial community structure was assessed using terminal-restriction fragment length polymorphism (T-RFLP) community

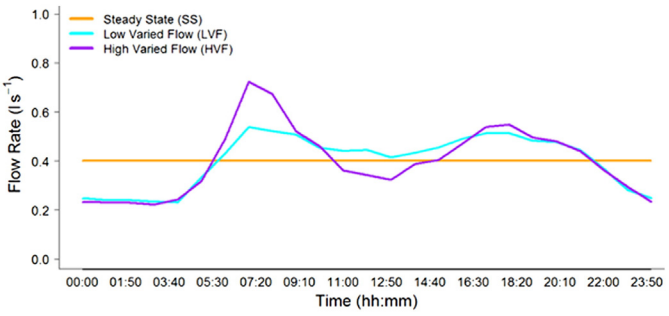

Fig. 2. Daily flow patterns of the hydraulic regimes used in this study. All regimes had the same average total daily flow rate (0.4 ls^{-1}) and shear stress (0.30 Nm^{-2}), which is the average flow rate in UK DWDS for 75–100 mm diameter pipes (Husband et al., 2008).

fingerprinting (Osborn et al., 2000) of bacterial 16S rRNA genes, according to the protocol detailed in Fish et al. (2015). In brief, biofilm was removed from the Day 28, Post-flush and Day 0 outer coupons (n = 9, and n = 3 controls) by brushing into 30 ml sterile PBS and filtering the suspension through a 47 mm diameter, 0.22 μm pore nitrocellulose membrane. DNA was extracted from the membrane using the proteinase K chemical lysis method (Zhou et al., 1996) with CTAB (hexadecyltmethyl ammonium bromide) incubation. Bacterial 16S rRNA genes were amplified by PCR using the primers 63F which was labelled with 6′ carboxyfluorescein dye (6-FAM-CAGGCCTAACACATGCAAGTC) and 518R (CGTATTACCGCGGCTGCTCG) (Girvan et al., 2003) – reaction and cycling conditions as described in Fish et al. (2015) Bacterial amplicons were digested with 10 U of *Alu*I (Roche, Germany), as preliminary tests showed *Alu*I to be more discriminatory than *Cfo*I. Amplicons were desalted and denatured with hi-di formamide containing 0.5% GeneScan™500 ROX™ internal size standard (Applied Biosystems, Warrington, UK). Samples and controls were electrophoresed using an ABI 3730 PRISM® capillary DNA analyser with POP7 (denaturing) polymer.

T-RFLP electropherograms were analysed using GeneMapper® v3.7 (Applied Biosystems) to establish the size of each T-RF using the Local Southern method (with reference to the size standards). For each fingerprint profile the peak area and size of each T-RF was aligned using T-Align (Smith et al., 2005) (confidence interval 0.5 nt), then normalised to exclude fragments that were <0.5% of the community profile. PRIMER-E v6.1 (Clarke, 1993) was used for multivariate analysis, which included hierarchical clustering and nMDS plots. Ecological parameters were calculated relative to the profiles: richness, diversity (using Shannon's index) and evenness (using Pielou's index).

2.5. Statistical analysis

Due to differences in the nature of the various datasets a range of statistical tests were applied, in all cases p-values (significance level was <0.05) are reported where relevant, along-side any other relevant values specific to each test.

Physical structure parameters were not normally distributed, therefore they were compared using non-parametric statistics, specifically Kruskal-Wallis (for comparison of >2 datasets, df = 2 in all cases, χ^2 values presented in results) or Wilcoxon (for comparison of two datasets, W values reported).

Bacterial community structures were compared using the multivariate statistical tests Analyses Of Similarity (ANOSIM: global-R values presented) and similarity percentages (SIMPER). Ecological indices were compared statistically using ANOVA (for >2 datasets, df = 2 in all cases, where p-values were significant a Tukey HSD test was subsequently applied) or a *t*-test (for comparison of two datasets, *t* values reported).

3. Results

3.1. Effect of hydraulic regime upon biofilms after 28 days of growth

3.1.1. Water quality

Regular water sampling across the experiments showed full compliance with UK standards (Table S1) and no substantial differences therein (tested using Kruskal Wallis or Wilcoxon tests) such that the greatest variation between experiments was the hydraulic regime.

3.1.2. Biofilm physical structure

The triple staining CLSM analysis revealed that under each flow regime, biofilms were morphologically heterogenic, with cells, carbohydrates and proteins generally detectable in individual FOV but not completely co-localised (e.g. Fig. 3). Biofilm volumes ($\mu m^3/\mu m^2$) were greater at Day 28 than at Day 0. Average (median) total biofilm volume increased by five-times under SS (Day 0 = 120 $\mu m^3/\mu m^2$, Day 28 = 600 $\mu m^3/\mu m^2$), 36-times under LVF (Day 0 = 2 $\mu m^3/\mu m^2$, Day 28 = 76 $\mu m^3/\mu m^2$) and 45-times under HVF (Day 0 = 9 $\mu m^3/\mu m^2$, Day 28 = 409 $\mu m^3/\mu m^2$), with SS Day 28 biofilms having the greatest total biomass.

At Day 28, LVF biofilms had the lowest volume of cells, carbohydrates or proteins (Fig. 3), whereas SS and HVF biofilms had similar volumes of cells and proteins, but carbohydrates were significantly greater in SS (Fig. 3B). Spread (a proxy for thickness) and peak location (the Z-position of the maximum area covered, i.e. greatest density, of a particular component) were calculated to determine the distributions of the cells, carbohydrates and proteins throughout the biofilms (Table 1; Fig. S1). At Day 28, LVF biofilms had significantly lower cell and protein spreads ($W \le 436.0$, $p \le 0.0454$) than SS or HVF biofilms (Table 1), following the trends in volume (reduced volume equated to a lower spread). In Day 28 LVF biofilms, the carbohydrate spread was similar to SS ($W = 252.0$, $p = 0.2467$) but greater than HVF ($W = 172.0$, $p = 0.0099$), despite HVF having a greater carbohydrate volume, indicative of an increased carbohydrate density over a narrower depth in HVF than LVF biofilms. Hydraulic regime did not affect the peak location of carbohydrates or proteins ($\chi^2 \ge 1.83$, $p \ge 0.1099$) which generally occurred above that of the cells, nearer the biofilm-water interface (Fig. S1). At Day 0, there were no differences in the spread or peak location of any stained component within biofilms from each regime ($\chi^2 \ge 1.97$, $p \ge 0.1167$).

Irrespective of hydraulic regime, Day 28 biofilms were dominated by EPS rather than cells (EPS-to-cell ratio in Table 1). LVF biofilms had the lowest EPS volume but a significantly higher proportion of EPS per volume of cells than the SS or HVF biofilms ($W \le 105.0$, $p < 0.0001$; Table 1), which did not differ significantly from each other ($W = 378.0$, $p = 0.063$). The EPS-to-cell ratios at Day 0 biofilms were consistently <1, demonstrating the predominance of cells over EPS and there was no difference between the hydraulic regimes ($\chi^2 = 0.26$, $p = 0.8786$).

At Day 28, regardless of hydraulics, the EPS was predominantly comprised of carbohydrate (carbohydrate-to-protein ratios all >1; Table 1). However, proteins accounted for an increasing proportion of the EPS volume following the sequence SS < HVF < LVF, with LVF biofilms being significantly different from SS ($W = 411.0$, $p = 0.0285$).

3.1.3. Bacterial community structure and diversity

Irrespective of hydraulics, biofilm bacterial communities were more complex at Day 28 than Day 0: a greater total number of different bacterial terminal-restriction fragments (T-RFs) were detected within Day 28 profiles (SS = 102, LVF = 122, HVF = 104) than at Day 0 (SS = 6, LVF = 13, HVF = 4) and relative richness and diversity both increased (Table 2).

Fig. 4A shows that at Day 0, biofilm bacterial community structure was very similar between the hydraulic regimes as the samples formed a single cluster (aside from one outlier from SS). However, at Day 28, community structure varied significantly between the regimes, with SS forming a single cluster that was distinct (global-$R \ge 0.865$, $p < 0.0001$; average dissimilarity ≥84%) from the two VF communities (Fig. 4), which did not differ significantly from each other (global-$R = 0.069$, $p = 0.1800$). Day 28 LVF communities had a lower relative richness (ANOVA: $p = 0.0128$; Tukey: $p = 0.0109$), diversity (ANOVA: $p = 0.0081$; Tukey: $p = 0.0067$) and evenness (ANOVA: $p = 0.0055$; Tukey: $p = 0.0056$) than SS communities but the ecological indices of LVF and HVF biofilms did not differ significantly.

SIMPER analysis demonstrated that the majority (60%) of the variation between the SS and LVF or HVF communities was attributed to 37 T-RFs (8 exclusive to LVF, 10 exclusive to SS, 19 shared) or 33 T-RFs (7 exclusive to SS, 7 exclusive to HVF, 19 shared), respectively. The shared T-RFs were present in biofilms from both the compared regimes but at different relative abundances.

Although LVF and HVF communities did not differ significantly they had an average of 63% dissimilarity, explained by 33 T-RFs, of which 28 were common to both, but present at different relative abundances.

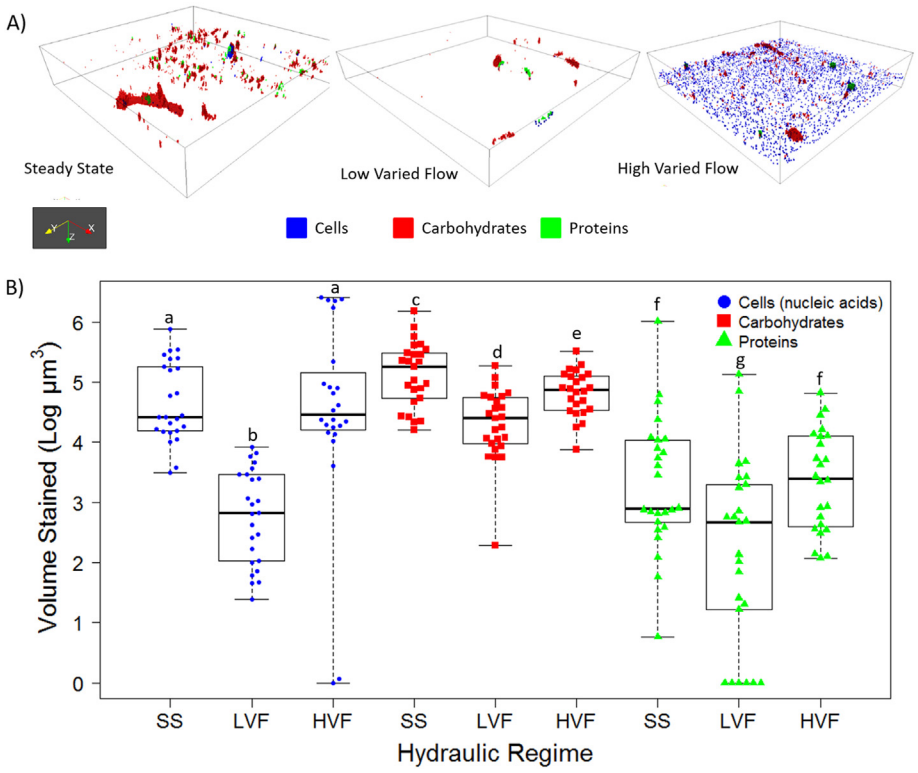

Fig. 3. Effect of hydraulic regime on distribution of cells, carbohydrates and proteins within Day 28 biofilms. SS = Steady State, LVF = Low Varied Flow, HVF = High Varied Flow. A) 3D projection of example SS, LVF and HVF Day 28 biofilms; plotting regions shown are 420 μm × 420 μm × 94.4 μm, 420 μm × 420 μm × 63.5 μm and 420 μm × 420 μm × 98.7 μm, respectively. B) Variation in volume of cells, carbohydrates and proteins within biofilms. Data are logged. Each data point represents a different FOV (n = 25 for SS and LVF, n = 24 for HVF). Box and whisker plots show the range, interquartile range and median – indicated by the solid black line. For each biofilm component (cells, carbohydrates and proteins), plots with different letters are significantly different from each other (W ≤ 616.0, p ≤ 0.034).

3.2. Responses to imposing elevated shear stress

3.2.1. Water quality response

During the flushing phase of each of the hydraulic experiments the only detectable, significant and consistent water quality changes were increases in the iron and manganese concentrations (Fig. 5). Flushing of the LVF biofilms resulted in lower increases in both iron (average increase of 13.11 μg l^{-1}) and manganese (average increase of 2.86 μg l^{-1}) concentrations in water than occurred during the flushing of the HVF (average increase of 30.56 μg iron l^{-1} and 7.00 μg manganese l^{-1}) or SS (average increase of 48.89 μg iron l^{-1} and 7.78 μg manganese l^{-1}) biofilms.

3.2.2. Biofilm physical structure response

Flushing did not remove all the biofilm nor did it result in a homogenous Post-flush structure; cells, carbohydrates and proteins were detectable in biofilms across the three regimes Post-flush, but the SS, LVF and HVF biofilms were different from each other (Fig. 6).

Day 28 and Post-flush biofilms were compared for each hydraulic regime to determine any changes in physical structure due to flushing. No changes were detected in cell volume or spread for any regime (W ≥ 281, p ≥ 0.3569; Table 1). Carbohydrate volume and spread decreased during the flushing of the LVF biofilms (W ≥ 168, p ≤ 0.0026) but no significant differences were found for SS or HVF biofilms (W ≥ 243, p ≥ 0.2611). Protein volume and spread decreased significantly in all three hydraulic regimes during the flushing phase (W ≤ 206, p ≤ 0.0465; Table 1). The volumes presented are per μm^2, a far smaller surface area than that of the pipelines being flushed (~50 m^2), therefore the biofilm volumes attached/mobilised from each pipeline would be many magnitudes greater (1 $m^2 = 10^{12}$ μm^2).

For SS and LVF conditioned biofilms, the detachment of the EPS, particularly proteins, led to a decrease in the EPS-to-cell ratio Post-flush compared to Day 28 (Table 1, only significant for LVF; W = 494, p =

Table 1
Volume ratios and spread values of stained cells, carbohydrates and proteins (EPS) in Day 28 and Post-flush drinking water biofilms from each hydraulic regime (average shown is the median).

Hydraulic regime	Ratio[A] (AU)				Spread (μm)					
	EPS[B]:cells		Carbohydrates:proteins		Cells		Carbohydrates		Proteins	
	Day 28	Post-flush	Day 28	Post-flush	Day 28	Post-flush	Day 28	Post-flush	Day 28	Post-flush
SS	4.9	11.4	62.3	2977.6[C]	25.70	21.43	24.91	21.69	26.30	16.60
LVF	26.4	4.4	14.2	286.6[C]	20.12	18.66	24.95	21.21	16.49	ND[D]
HVF	2.0	1.7	33.2	75.5[C]	25.09	22.02	20.30	20.28	21.97	17.04

[A] The first component is divided by the second; a value >1 indicates a greater volume of the first component; a value <1 indicates a greater volume of the second component.
[B] EPS volume was calculated for each field of view (FOV) by summing the carbohydrate and protein volumes. SS = Steady State, LVF = Low Varied Flow, HVF = High Varied Flow.
[C] Due to protein volumes being undetected in some FOV, these ratios could not be calculated in some instances so replication for SS, LVF and HVF is n = 21, n = 9, n = 23, respectively.
[D] ND = not detected; proteins could not be detected in several FOV but where proteins were detected (n = 9) the median spread was 7.68 μm.

Table 2
Ecological diversity indices of the bacterial communities of biofilms from each hydraulic regime at Day 0, Day 28 and Post-flush; data shown is the mean (and standard deviation), calculated from the relative abundance data of T-RFLP analysis of 16S rRNA genes.

Hydraulic Regime	Relative richness[A]			Relative diversity[B]			Relative evenness[C]		
	Day 0	Day 28	Post-flush	Day 0	Day 28	Post-flush	Day 0	Day 28	Post-flush
SS	3 & 5[D]	37 (5)	19 (9)	1.04 & 1.43[D]	3.48 (0.13)	2.76 (0.46)	0.89 & 0.95[D]	0.97 (0.01)	0.96 (0.02)
LVF	6 (2)	26 (8)	7 (6)	1.50 (0.32)	3.04 (0.36)	1.38 (0.88)	0.87 (0.04)	0.94 (0.02)	0.86 (0.07)
HVF	2 (1)	30 (7)	10 (7)	0.51 (0.47)	3.20 (0.27)	1.92 (0.87)	0.78 (0.08)	0.95 (0.02)	0.90 (0.08)

[A] Number of T-RFs.
[B] Shannon's index.
[C] Pielou's index.
[D] 16S rRNA genes could only be amplified from 2/9 samples, so an average could not be calculated, SS = Steady State, LVF = Low Varied Flow, HVF = High Varied Flow.

0.0002). Subsequently, Post-flush SS and LVF biofilms had EPS matrices with a significantly greater carbohydrate proportion (Table 1) than at Day 28 ($W \geq 59$, $p \leq 0.0380$). No significant differences were detected between the HVF carbohydrate-to-protein-ratios ($W = 231$, $p = 0.4224$). The peak locations of the proteins and carbohydrates were generally unaffected by the flushing, regardless of conditioning hydraulics ($W \geq 270.5$, $p \geq 0.0533$) the Post-flush EPS peaks remained above that of the cells (Fig. S2).

3.2.3. Bacterial community structure and diversity responses

Post-flush, the SS, LVF and HVF biofilm bacterial community structures all differed (Fig. 4B; global-R = 0.536, $p < 0.0001$) and replicates within a treatment were more divergent than at Day 28, indicating an increase in the heterogeneity in response to elevated shear stress. In contrast to Day 28, the Post-flush LVF and HVF biofilm communities differed significantly (global-R = 0.246, $p = 0.022$) with an average of 85.38% dissimilarity, which was driven by 12 T-RFs, 7 of which were common to the communities of both regimes but present at different relative abundances.

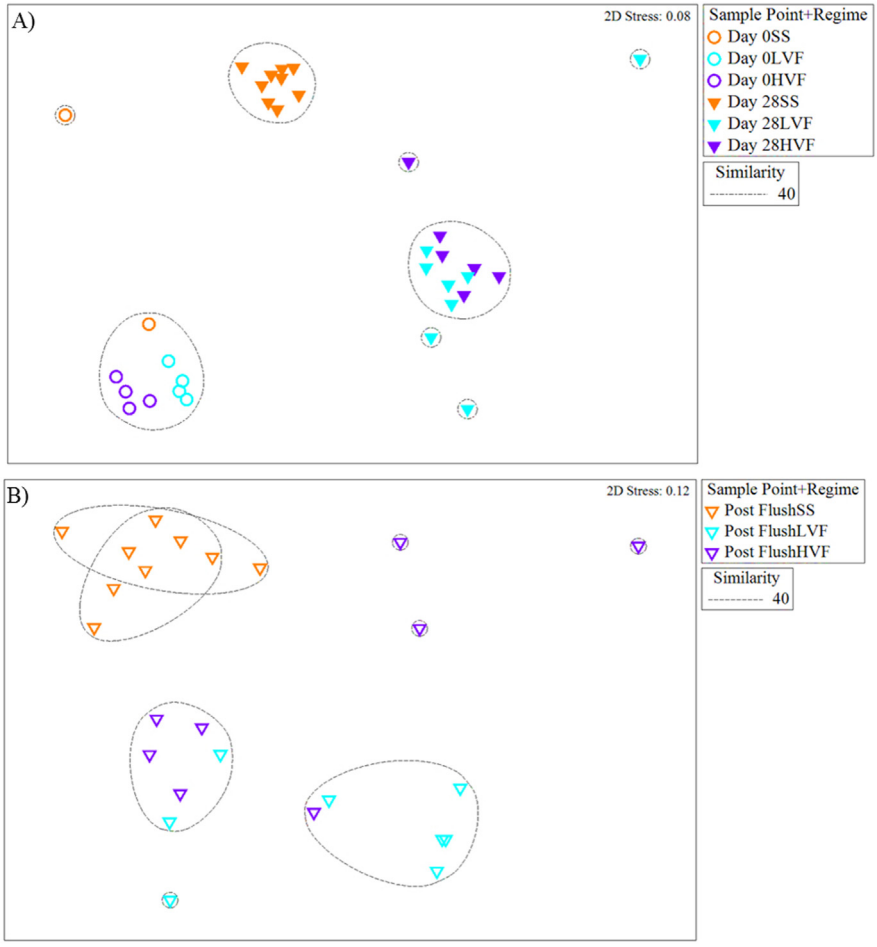

Fig. 4. Variation in bacterial community structure of biofilms developed under the SS, LVF or HVF hydraulic conditions. A) Growth phase (Day 0 vs. Day 28). B) Post-flush. nMDS plots shown were generated from relative abundance of T-RFs of 16S rRNA genes, analysed using Bray-Curtis similarity and cluster analysis. Similar plots were observed on analysis of T-RF presence/absence data (data not shown) Black lines indicate clusters of at least 40% similarity, based on group averages from hierarchical clustering analysis.

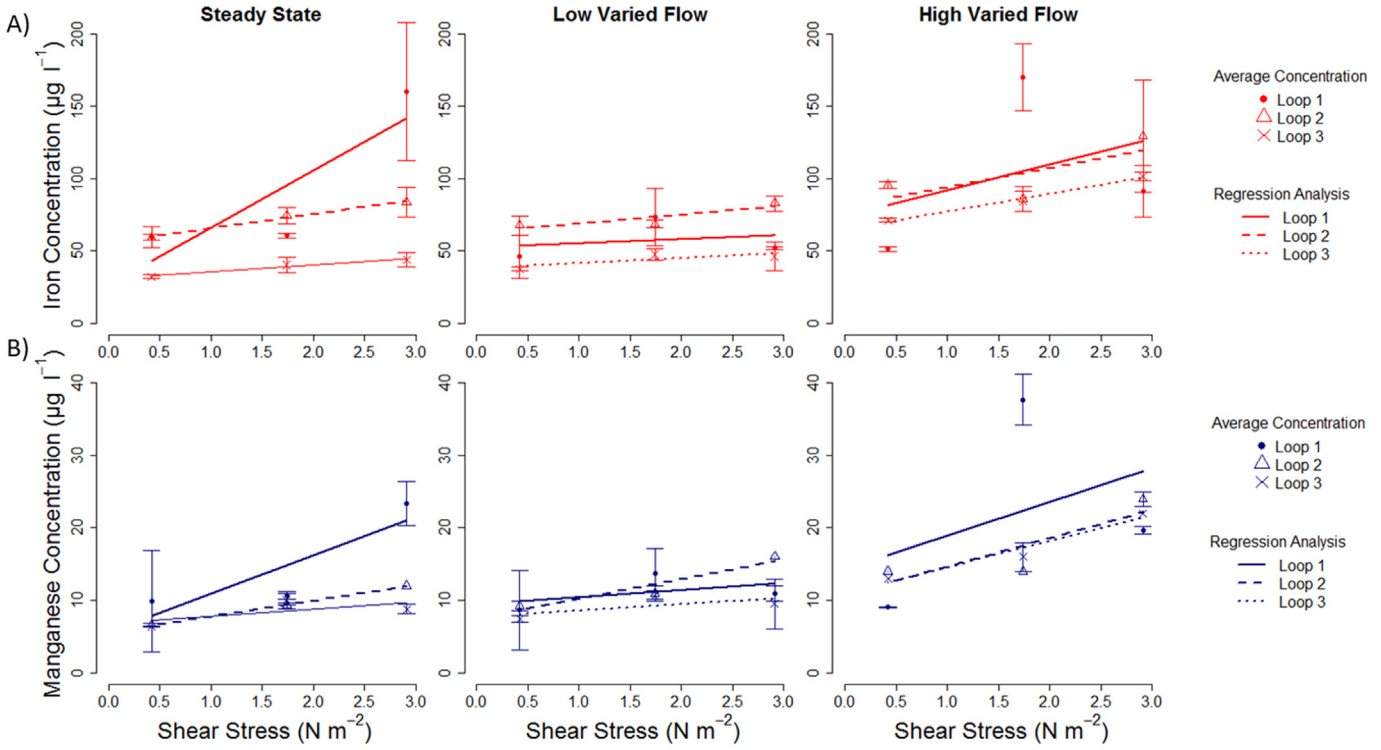

Fig. 5. Concentrations of A) iron and B) manganese during the flushing phase of biofilms developed under SS, LVF and HVF conditions. The average (n = 3) concentrations (±one standard deviation) at the end of one turnover of each of the three flushing steps are plotted. As each loop had to be flushed separately, the data is normalised to the mixing phase and plotted for each independently; the details of the regression analysis are presented in Table S2.

Irrespective of hydraulic regime, a lower total number of different bacterial T-RFs was detected Post-flush (SS = 101, LVF = 36, HVF = 38) than at Day 28 and bacterial richness ($t \geq 5.11$, $11 \leq df \leq 13$, $p \leq 0.0004$) and diversity ($t \geq 3.89$, $9 \leq df \leq 11$, $p \leq 0.0039$) significantly reduced (Table 2). This shift did not significantly affect the relative evenness of the SS or HVF communities but the LVF Post-flush communities

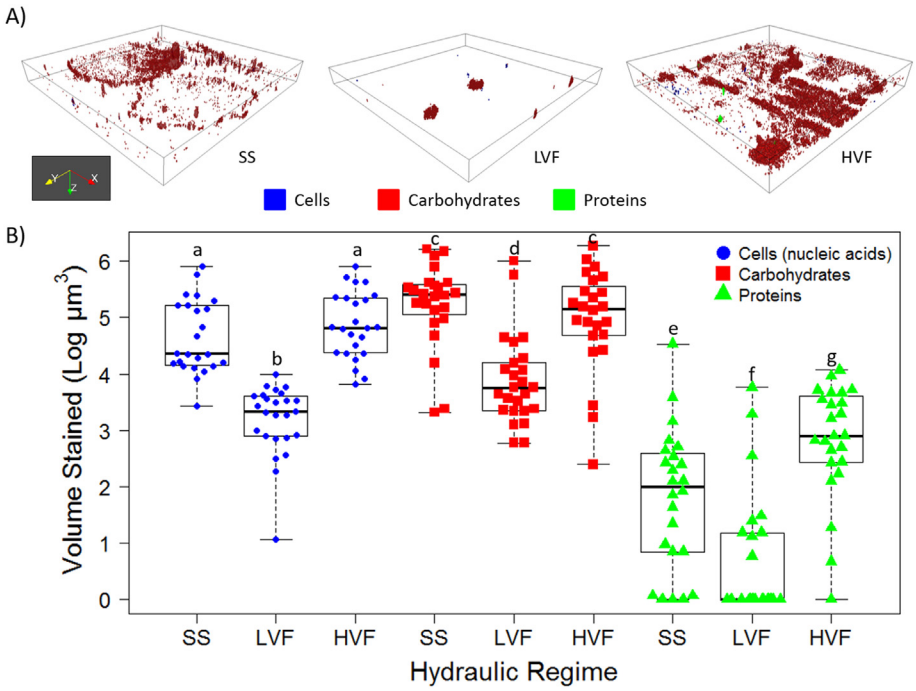

Fig. 6. The effect of hydraulic regime upon the cells, carbohydrates and proteins within Post-flush biofilms. SS = Steady State, LVF = Low Varied Flow, HVF = High Varied Flow. A) 3D projection of example SS, LVF and HVF Day 28 biofilms, plotting regions shown are 420 µm × 420 µm × 47.0 µm, 420 µm × 420 µm × 37.6 µm and 420 µm × 420 µm × 61.1 µm, respectively. B) Volume is logged to show all data on the same scale. Each data point represents a different FOV (n = 24 for SS and HVF, n = 25 for LVF). Box and whisker plots show the range, interquartile range and median – indicated by the solid black line. For each biofilm component (cells, carbohydrates and proteins), plots with different letters are significantly different ($W \leq 588.0$, $p \leq 0.0013$).

experienced a significant decrease ($t = 3.31$, df = 10, $p = 0.0078$). SS Day 28 and Post-flush communities differed significantly (global-R = 0.313, $p = 0.0001$) with 58.83% dissimilarity according to SIMPER, which was explained by 31 T-RFs of which 30 were common to both sample points, indicating a reduction in the abundance of certain T-RFs, rather than removal of T-RFs in response to the flushing. LVF bacterial communities also differed before and after flushing (global-R = 0.451, $p = 0.0040$) with Day 28 and Post-flush communities having an average dissimilarity of 85.45%, driven by 21 T-RFs, 12 of which were common at each sample point (6 were unique to Day 28 biofilms and 3 to Post-flush). The HVF biofilm bacterial community structure was unaffected by the flushing (global-R = 0.072, $p = 0.1590$), despite the changes in ecological indices. This may indicate the removal of rarer T-RFs which would lower the richness and diversity but not affect the overall structure of the community to make a significant change when compared to Day 28.

4. Discussion and conclusions

This study presents the first exploration of the interactions between hydraulic pattern and DWDS biofilms, importantly incorporating both EPS and cell analysis. Previous studies have generally investigated the impact of different constant flow velocities upon biofilms (Lemos et al., 2015; Möhle et al., 2007; Purevdorj et al., 2002; Wagner et al., 2009; Wang et al., 2014), rather than VF patterns. However, the findings herein demonstrate that after 28 days of development biofilm physical and community structure clearly differed between SS and VF regimes. Therefore, average flow rate, which was conserved across the three regimes, was not the primary selective pressure driving biofilm characteristics and hydraulic pattern exerted a significant conditioning force. This highlights the importance of accurately replicating DWDS hydraulics if results are to be real-world applicable.

Compared to the VF regimes, SS facilitated the accumulation of greater volumes of biomass likely because the biofilms experienced no hydraulic variation and therefore growth/development was undisturbed. Studies of wastewater (Wagner et al., 2009) or activated sludge fed (2007) biofilms and cell accumulation within the DWDS test facility at Sheffield (Sharpe, 2012) have also shown that lower flow rates or shear stresses (different steady states were tested) resulted in thicker biofilms. The unvarying shear stress of the SS regime also promoted the formation of a more complex, diverse biofilm bacterial community (indicated by ecological indices) that was distinct from those observed under VF conditions. Bacterial communities of freshwater (Rickard et al., 2004) and industrial-water biofilms (Rochex et al., 2008) have also been reported to be more diverse when developed under lower shear stresses. Conversely, Douterelo et al. (2013) did not detect differences between the bacterial communities of SS and VF conditioned biofilms. However, Douterelo et al. (2013) (and others previously using the DWDS test facility (Sharpe, 2012)) tested different hydraulic regimes simultaneously with a shared reservoir water supply, which would impose mixing-effects and seeding/cross-contamination between conditions. In the study presented herein, this was been addressed by running each condition independently. Our results suggest that, compared to the VF regimes, there was less selection pressure on SS biofilms, consequently, less EPS-per-cell was produced (particularly in comparison to LVF) and bacterial communities were more diverse.

If the SS trends were to hold true for comparison of the LVF and HVF biofilms it would be expected that LVF biofilms, which experienced less hydraulic variation than HVF, would have greater amounts of biofilm but less EPS per cell than HVF biofilms. However, the reverse was true, LVF limited biofilm accumulation, reducing bacterial diversity but promoting EPS production per cell whereas HVF was associated with increased biomass and bacterial diversity but less EPS per cell. The EPS composition of LVF and HVF biofilms also differed. Carbohydrates were the dominant component of all the biofilms, as has been reported in other environments (Simões et al., 2005; Wagner et al., 2009), but LVF Day 28 biofilms had a greater proportion of proteins in their EPS than HVF (or SS), suggesting that protein synthesis was promoted. Hydraulic and protein interactions have not been fully explored for DWDS biofilms. Studies in other environments have recorded both negative (Wagner et al., 2009) and positive (Simões et al., 2005) correlations between protein concentrations and flow rates/velocity. The trends discussed between the physical structure of the LVF and HVF biofilms are unexpected. However, a discolouration study by Sharpe (2012) also found that HVF promoted cell accumulation (only cells were analysed) compared to LVF and as the two regimes were tested simultaneously any seasonal affects can be discounted. Therefore, it can be concluded that the patterns in biofilm structures are a true consequence of hydraulic conditioning, although the exact processes driving the differentiation in EPS and cell accumulation are not yet clear.

The development of greater biomass volumes at HVF than LVF could be attributed to greater mass-transfer of trace inorganics and organics (including cells) to the pipe-wall because of greater turbulence. Industrial water-fed (Rochex et al., 2008), single-species (Dunsmore et al., 2002) and non-chlorinated drinking water-fed (Sly et al., 1988) reactor biofilms have been found to accumulate more material under more turbulent conditions, supporting this theory. However, with the DWDS biofilms in this study, this seems unlikely because LVF and HVF flow rates were within 10% of each other for 14 h of each day. Furthermore, although HVF had the highest peak flow, in order to maintain the same total flow in 24 h the LVF had a higher flow rate than HVF for a total of 5:45 (hh:mm) compared to 4:34 (hh:mm), where the reverse was true.

Under HVF, the diurnal peak in shear stress could have cyclically removed material, consistently "resetting" the biofilm, promoting a younger physical structure with more cells but less EPS. Interestingly, the greatest area density (assessed by peak location) of the EPS occurred above that of the cells, i.e. nearer to the bulk-water, consistent with our prior observations (Fish et al., 2015). Potentially, the peak of the HVF removed the "top" layers of biofilm which had more EPS, leaving behind biofilms with a reduced EPS per cell content. While this theory would explain the (proportionally) less extensive matrix in HVF biofilms compared to LVF biofilms, it does not explain the greater volume of material under HVF conditions. Simões et al. (2005, 2003) found that less EPS (carbohydrates) formed per gram of biofilm under higher velocity conditions (0.532 ms^{-1} compared to 0.204 ms^{-1}) but respiratory activity was greater, indicating more cellular activity. Cellular activity was not measured in the current study but it is possible that greater cellular activity occurred within HVF than LVF biofilms, this could explain increasing cell replication/growth and material accumulation. It is also plausible that the increased EPS production in LVF depleted resources available for growth/replication or led to death of the EPS producing cells, further increasing the difference between LVF and HVF biofilm volumes. These results confirm the observations of Kreft and Wimpenny (2001) that EPS production reduces the growth of producers in a biofilm growth model study. They also observed that due to energy costs, the accumulation of EPS can decrease as synthesis rate increases (Kreft and Wimpenny, 2001). Our findings lend support to this for DWDS as HVF biofilms produced more EPS but accumulated less per cell volume. Potentially the EPS producers were expending energy on a matrix that was then cyclically removed but facilitated an increase in abundance of non-producers while it was intact.

Despite their different physical structures LVF and HVF Day 28 biofilm communities were very similar, indicative of a shared selection pressure upon community structure, although it is unclear whether the conditioning force was flow variation or the low flow-period. LVF and HVF communities were dominated by particular T-RFs (although these were in greater abundances under HVF), which may correspond to taxa that are better adapted to resisting variations in flow than others. For example, Rickard et al. (2004) found that freshwater biofilms grown within a high shear stress environment contained more auto-aggregating than co-aggregating bacteria, the former of which have

stronger interactions and are therefore more resistant to detachment. Elvers et al. (1998) established that less diverse populations produced thinner biofilms in photo-processing tanks and, in the current study, LVF biofilms were the thinnest and least diverse, confirming this trend for DWDS.

Unsurprisingly, at Day 28, regardless of hydraulics, EPS volumes exceeded cell volumes and bacterial community structure was more complex than at Day 0 (especially for SS biofilms); these patterns are commonly observed as biofilms mature(Rochex et al., 2008; Wagner et al., 2009). However, hydraulic regime appeared to influence the rate of DWDS biofilm maturation, a phenomenon also reported by Rochex et al. (2008) who analysed reactor biofilms developed under different steady state shear stresses (0.055–0.27 Pa). Biofilm development follows a sequence of: primary/secondary adhesion, where diversity is high and EPS synthesis begins; initial growth, where diversity reduces due to increased competition and EPS production increases; and maturation, where EPS is more developed providing a range of niches and so diversity increases (Fish et al., 2016). Accordingly, although only developed for a month, SS biofilms could be described to be the most developed biofilms in this study, progressing the most towards the maturation stage and supporting the most diverse community, followed by the LVF biofilms which had the least bacterial diversity but the most EPS per cell and finally the HVF biofilms which were the least developed, with greater diversity than the LVF biofilms but the lowest EPS:cell ratio.

Previous studies have shown that higher turbulence or shear stress conditions during development resulted in biofilms that were more resistant to detachment (Ohashi et al., 1999; Paul et al., 2012; Percival et al., 1999; Wang et al., 2014) but these findings are based upon conditioning biofilms to steady state hydraulics in reactors or flumes. Here, we found that regardless of conditioning hydraulics, bulk-water iron and manganese concentrations increased during the flushing phase, indicative of discolouration, but that the greatest increase was generated under SS conditions. This trend has been previously observed at 8 °C (Sharpe, 2012); systems that were conditioned to a 0.8 ls^{-1} steady state flow had a greater discolouration response than systems conditioned to a VF regime, which had a peak flow of 0.8 ls^{-1}. These results indicate that flow variation is more important than a high flow in limiting discolouration and further demonstrate the need for research to replicate and better understand DWDS hydraulics.

LVF conditions generated less discolouration than HVF, which could be attributed to reduced EPS mobilisation and/or less prior incorporation of iron/manganese into the EPS of LVF biofilms. Less iron and manganese were found under 0.01 ms^{-1} than at 0.50 ms^{-1} in a reactor-based study (Sly et al., 1988) but this previous finding cannot be assessed for the DWDS biofilms as inorganics at the pipe-wall were not quantified. Abe et al. (2012) found that biofilms developed under lower shear stresses had greater mechanical strength and were more resistant to detachment, potentially due to differences in EPS, governed by the hydraulics during development. LVF biofilms had the greatest EPS-to-cell ratio and an extensive spread of carbohydrate, they also experienced the lowest difference in EPS volume before and after flushing. This observation could be a function of the reduced biofilm accumulation in LVF Day 28 biofilms (so less material is present to be mobilised) and/or greater adhesion due to the more extensive EPS. Critically, prior DWDS biofilm research has rarely quantified the proteins, which has significant implications when categorising a biofilm as “stable”; cells or carbohydrates may be unaffected by increased external forces but this does not necessarily mean a biofilm is “stable” - other components may have been detached at detectable levels. Picioreanu et al. (2000) found that increased biofilm growth rate correlated with detachment events, possibly because microorganisms preferentially used energy in cell replication rather than EPS production and therefore were more weakly adhered. Potentially the HVF biofilms, which experienced a higher growth rate than LVF, had a greater propensity to detach, thus presenting a greater discolouration risk.

Although a change in cell volume was not detected during flushing, bacterial communities (regardless of hydraulic regime) decreased in their relative richness and diversity, indicating the loss of taxa and a shift towards a more specialised community, likely better able to resist detachment. Bacterial communities were the most stable in HVF biofilms, experiencing no significant changes in structure despite the changes in ecological indices, suggesting that rarer T-RFs were detached which had low relative abundance. Möhle et al. (2007) also found very little change in the bacterial (and carbohydrate) contents of municipal wastewater biofilms developed under higher shear stress (0.037 Nm^{-2} within a rotating disc reactor) before and after gauging. In contrast, Douterelo et al. (2013) detected differences in the HVF bacterial community both pre- and post-flush, with members of the Proteobacteria increasing, in particular. Possibly the greater sensitivity of sequencing compared to fingerprinting techniques detected these subtle changes or the potential for cross-seeding between regimes in the earlier study (previously discussed) masked the similarities presented herein. Interestingly, at Day 28 the LVF and HVF bacterial communities were similar to each other but Post-flush they were significantly different. Biofilms from the two regimes had different physical structures, therefore it is concluded that different EPS characteristics, due to different hydraulic conditioning, caused the two communities to respond differently to elevated shear stress.

Post-flush biofilms did not have a homogenous structure across the three regimes but a strongly adhered layer of (predominantly) carbohydrate with cells was consistently observed. The persistence of a strongly adhered biofilm base layer has been well documented in bench-top scale studies (Abe et al., 2012; Lemos et al., 2015; Möhle et al., 2007; Ohashi et al., 1999; Paul et al., 2012; Simões et al., 2005; Staudt et al., 2004), some of which also established that this layer had a high carbohydrate concentration, possibly because these molecules are central to mechanical stability. However, many studies did not investigate proteins so it is not possible to ascertain if the protein or carbohydrate content contributed more to the EPS. A continued biofilm presence Post-flush provides an alternative surface for microbial attachment which may facilitate the incorporation of secondary colonisers into the biofilm and provide an additional source of nutrients to the cells remaining attached.

In conclusion, the complex patterns observed herein demonstrate that there is no simple, linear relationship between hydraulic regime, biofilm characteristics and discolouration. However, hydraulics did condition for different biofilm structures, which subsequently present different discolouration risks, with SS biofilms being distinct from VF. This demonstrates the need for future biofilm research to focus on the impact of hydraulic pattern and not just on absolute flow rate and highlights issues with extrapolating trends from studies using SS regimes to real DWDS. Hydraulic pattern had a greater impact upon EPS than on the composition of the microbial community synthesising it, therefore monitoring the pipeline environment is crucial to predict the discolouration risk that a biofilm may present. Flushing did not completely remove biofilms but the biofilm bacterial community structure did vary between the hydraulic regimes; HVF biofilms had the most stable community structure but the LVF regime conditioned for the lowest discolouration risk. It can be argued as to which biofilm characteristics are most desirable. While HVF presents a greater risk of discolouration if left unmonitored, the promotion of a younger biofilm with less EPS means that more material can be removed with targeted flushing, potentially leading to a cleaner pipeline. It could also be argued that promoting the presence of a younger biofilm may result in a biofilm structure more susceptible to disinfection agents as EPS is accredited with affording protection against disinfection.

Ultimately this study indicates that it is impossible to prevent biofilm accumulation within DWDS but that hydraulics could be used to predict biofilm behaviour or condition for “low-risk” biofilms, thus facilitating a move from reactive to pro-active management of DWDS biofilms and water quality.

Funding

KF was funded by a Natural Environment Research Council (NERC; http://www.nerc.ac.uk/) PhD studentship (NE/H52489X/1) and supported by the Pennine Water Group EPSRC Platform Grant (EP/1029346/1). The research was conducted within the Pipe Dreams project, supported by the U.K. Engineering and Physical Sciences Research Council (EPSRC; http://www.epsrc.ac.uk/) Challenging Engineering: EP/G029946/1. Funders had no role in study design, sample collection, data analysis or manuscript preparation. DNA extraction and bacterial community fingerprinting was performed at the NERC Biomolecular Analysis Facility (NBAF) at Sheffield (http://nbaf.nerc.ac.uk/) and supported by NERC, UK.

Appendix A. Supplementary data

Supplementary data to this article can be found online at http://dx.doi.org/10.1016/j.scitotenv.2017.03.176.

References

Abe, Y., Skali-Lami, S., Block, J.-C., Francius, G., 2012. Cohesiveness and hydrodynamic properties of young drinking water biofilms. Water Res. 46:1155–1166. http://dx.doi.org/10.1016/j.watres.2011.12.013.

Beyenal, H., Lewandowski, Z., 2002. Internal and external mass transfer in biofilms grown at various flow velocities. Biotechnol. Prog. 18:55–61. http://dx.doi.org/10.1021/bp010129s.

Böckelmann, U., Janke, A., Kuhn, R., Neu, T.R., Wecke, J., Lawrence, J.R., Szewzyk, U., 2006. Bacterial extracellular DNA forming a defined network-like structure. FEMS Microbiol. Lett. 262:31–38. http://dx.doi.org/10.1111/j.1574-6968.2006.00361.x.

Boxall, J., Saul, A., 2005. Modeling discoloration in potable water distribution systems. J. Environ. Eng. ASCE 131:716–725. http://dx.doi.org/10.1061/(ASCE)0733-9372(2005)131:5(716).

Clarke, K.R., 1993. Non-parametric multivariate analyses of changes in community structure. Aust. J. Ecol. 18:117–143. http://dx.doi.org/10.1111/j.1442-9993.1993.tb00438.x.

Deines, P., Sekar, R., Husband, P., Boxall, J., Osborn, A., Biggs, C., 2010. A new coupon design for simultaneous analysis of in situ microbial biofilm formation and community structure in drinking water distribution systems. Appl. Microbiol. Biotechnol. 87:749–756. http://dx.doi.org/10.1007/s00253-010-2510-x.

Douterelo, I., Sharpe, R.L., Boxall, J.B., 2013. Influence of hydraulic regimes on bacterial community structure and composition in an experimental drinking water distribution system. Water Res. 47:503–516. http://dx.doi.org/10.1016/j.watres.2012.09.053.

Dunsmore, B., Jacobsen, A., Hall-Stoodley, L., Bass, C., Lappin-Scott, H., Stoodley, P., 2002. The influence of fluid shear on the structure and material properties of sulphate-reducing bacterial biofilms. J. Ind. Microbiol. Biotechnol. 29:347–353. http://dx.doi.org/10.1038/sj.jim.7000302.

Elvers, K.T., Leeming, K., Moore, C.P., Lappin-Scott, H.M., 1998. Bacterial-fungal biofilms in flowing water photo-processing tanks. J. Appl. Microbiol. 84:607–618. http://dx.doi.org/10.1046/j.1365-2672.1998.00388.x.

Fish, K.E., Collins, R., Green, N.H., Sharpe, R.L., Douterelo, I., Osborn, A.M., Boxall, J.B., 2015. Characterisation of the physical composition and microbial community structure of biofilms within a model full-scale drinking water distribution system. PLoS One 10, e0115824. http://dx.doi.org/10.1371/journal.pone.0115824.

Fish, K.E., Osborn, A.M., Boxall, J., 2016. Characterising and understanding the impact of microbial biofilms and the extracellular polymeric substance (EPS) matrix in drinking water distribution systems. Environ. Sci. Water Res. Technol. 2:614–630. http://dx.doi.org/10.1039/C6EW00039H.

Flemming, H.C., Wingender, J., 2001. Relevance of microbial extracellular polymeric substances (EPSs)–part I: structural and ecological aspects. Water Sci. Technol. J. Int. Assoc. Water Pollut. Res. 43, 1–8.

Flemming, H., Wingender, J., 2010. The biofilm matrix. Nat. Rev. Microbiol. 8:623–633. http://dx.doi.org/10.1038/nrmicro2415.

Gao, B., Zhu, X., Xu, C., Yue, Q., Li, W., Wei, J., 2008. Influence of extracellular polymeric substances on microbial activity and cell hydrophobicity in biofilms. J. Chem. Technol. Biotechnol. 83:227–232. http://dx.doi.org/10.1002/jctb.1792.

Ginige, M.P., Wylie, J., Plumb, J., 2011. Influence of biofilms on iron and manganese deposition in drinking water distribution systems. Biofouling 27:151–163. http://dx.doi.org/10.1080/08927014.2010.547576.

Girvan, M.S., Bullimore, J., Pretty, J.N., Osborn, A.M., Ball, A.S., 2003. Soil type is the primary determinant of the composition of the total and active bacterial communities in arable soils. Appl. Environ. Microbiol. 69:1800–1809. http://dx.doi.org/10.1128/AEM.69.3.1800-1809.2003.

Husband, P.S., Boxall, J.B., Saul, A.J., 2008. Laboratory studies investigating the processes leading to discolouration in water distribution networks. Water Res. 42:4309–4318. http://dx.doi.org/10.1016/j.watres.2008.07.026.

Husband, S., Fish, K.E., Douterelo, I., Boxall, J., 2016. Linking discolouration modelling and biofilm behaviour within drinking water distribution systems. Water Sci. Technol. Water Supply http://dx.doi.org/10.2166/ws.2016.045 ws2016045.

Ivleva, N., Wagner, M., Horn, H., Niessner, R., Haisch, C., 2009. Towards a nondestructive chemical characterization of biofilm matrix by Raman microscopy. Anal. Bioanal. Chem. 393:197–206. http://dx.doi.org/10.1007/s00216-008-2470-5.

Kreft, J.U., Wimpenny, J.W., 2001. Effect of EPS on biofilm structure and function as revealed by an individual-based model of biofilm growth. Water Sci. Technol. J. Int. Assoc. Water Pollut. Res. 43, 135–141.

Lehtola, M., Miettinen, I., Hirvonen, A., Vartiainen, T., Martikainen, P., 2006. Resuspension of biofilms and sediments to water from pipelines as a result of pressure shocks in drinking water distribution system. IWA Biofilm Systems IV. IWA-International Water Association, Amsterdam.

Lemos, M., Mergulhão, F., Melo, L., Simões, M., 2015. The effect of shear stress on the formation and removal of *Bacillus cereus* biofilms. Food Bioprod. Process. 93:242–248. http://dx.doi.org/10.1016/j.fbp.2014.09.005.

Möhle, R., Langemann, T., Haesner, M., Augustin, W., Scholl, S., Neu, T., Hempel, D., Horn, H., 2007. Structure and shear strength of microbial biofilms as determined with confocal laser scanning microscopy and fluid dynamic gauging using a novel rotating disc biofilm reactor. Biotechnol. Bioeng. 98:747–755. http://dx.doi.org/10.1002/bit.21448.

Neu, T., Lawrence, J., 2009. Extracellular polymeric substances in microbial biofilms. Microbial Glycobiology: Structures, Relevance and Applications. Elsevier, San Diego, pp. 735–758.

Ohashi, A., Koyama, T., Syutsubo, K., Harada, H., 1999. A novel method for evaluation of biofilm tensile strength resisting erosion. Water Sci. Technol. 39, 261–268.

Osborn, A.M., Moore, E.R.B., Timmis, K.N., 2000. An evaluation of terminal-restriction fragment length polymorphism (T-RFLP) analysis for the study of microbial community structure and dynamics. Environ. Microbiol. 2, 39–50.

Paul, E., Ochoa, J.C., Pechaud, Y., Liu, Y., Liné, A., 2012. Effect of shear stress and growth conditions on detachment and physical properties of biofilms. Water Res. 46:5499–5508. http://dx.doi.org/10.1016/j.watres.2012.07.029.

Percival, S., Knapp, J., Wales, D., Edyvean, R., 1999. The effect of turbulent flow and surface roughness on biofilm formation in drinking water. J. Ind. Microbiol. Biotechnol. 152–159.

Picioreanu, C., van Loosdrecht, M., Heijnen, J., 2000. Two-dimensional model of biofilm detachment caused by internal stress from liquid flow. Biotechnol. Bioeng. 72, 205–218.

Purevdorj, B., Costerton, J., Stoodley, P., 2002. Influence of hydrodynamics and cell signaling on the structure and behavior of *Pseudomonas aeruginosa* biofilms. Appl. Environ. Microbiol. 68:4457–4464. http://dx.doi.org/10.1128/AEM.68.9.4457-4464.2002.

R Development Core Team, 2008. R: A language and Environment for Statistical Computing. R Foundation for Statistical Computing, Vienna, Austria.

Rickard, A., McBain, A., Stead, A.T., Gilbert, P., 2004. Shear rate moderates community diversity in freshwater biofilms. Appl. Environ. Microbiol. 70, 7426–7435.

Rochex, A., Godon, J.-J., Bernet, N., Escudié, R., 2008. Role of shear stress on composition, diversity and dynamics of biofilm bacterial communities. Water Res. 42:4915–4922. http://dx.doi.org/10.1016/j.watres.2008.09.015.

Sharpe, R.L., 2012. Laboratory Investigations Into Processes Causing Discoloured Potable Water. The University of Sheffield.

Simões, M., Pereira, M., Vieira, M., 2003. Monitoring the effects of biocide treatment of *Pseudomonas fluorescens* biofilms formed under different flow regimes. Water Sci. Technol. 47, 217–223.

Simões, M., Pereira, M., Vieira, M., 2005. Effect of mechanical stress on biofilms challenged by different chemicals. Water Res. 39:5142–5152. http://dx.doi.org/10.1016/j.watres.2005.09.028.

Sly, L., Hodgkinson, M., Arunpairojana, V., 1988. Effect of water velocity on the early development of manganese-depositing biofilm in a drinking-water distribution-system. FEMS Microbiol. Ecol. 53, 175–186.

Smith, C.J., Danilowicz, B.S., Clear, A.K., Costello, F.J., Wilson, B., Meijer, W.G., 2005. T-Align, a web-based tool for comparison of multiple terminal restriction fragment length polymorphism profiles. FEMS Microbiol. Ecol. 54, 375–380.

Staudt, C., Horn, H., Hempel, D., Neu, T., 2004. Volumetric measurements of bacterial cells and extracellular polymeric substance glycoconjugates in biofilms. Biotechnol. Bioeng. 88:585–592. http://dx.doi.org/10.1002/bit.20241.

Vieira, M., Melo, L., 1999. Intrinsic kinetics of biofilms formed under turbulent flow and low substrate concentrations. Bioprocess Eng. 20, 369–375.

Vreeburg, J., Boxall, J., 2007. Discolouration in potable water distribution systems: a review. Water Res. 41:519–529. http://dx.doi.org/10.1016/j.watres.2006.09.028.

Wagner, M., Ivleva, N.P., Haisch, C., Niessner, R., Horn, H., 2009. Combined use of confocal laser scanning microscopy (CLSM) and Raman microscopy (RM): investigations on EPS - matrix. Water Res. 43:63–76. http://dx.doi.org/10.1016/j.watres.2008.10.034.

Wang, C., Miao, L., Hou, J., Wang, P., Qian, J., Dai, S., 2014. The effect of flow velocity on the distribution and composition of extracellular polymeric substances in biofilms and the detachment mechanism of biofilms. Water Sci. Technol. J. Int. Assoc. Water Pollut. Res. 69:825–832. http://dx.doi.org/10.2166/wst.2013.785.

Zacheus, O.M., Lehtola, M.J., Korhonen, L.K., Martikainen, P.J., 2001. Soft deposits, the key site for microbial growth in drinking water distribution networks. Water Res. 35:1757–1765. http://dx.doi.org/10.1016/S0043-1354(00)00431-0.

Zhou, J., Bruns, M.A., Tiedje, J.M., 1996. DNA recovery from soils of diverse composition. Appl. Environ. Microbiol. 62, 316–322.